Reassessment of the role of antiphase boundaries in the low-field magnetoresistance of Sr_2FeMoO_6

Tsang-Tse Fang*
Department of Materials Science and Engineering, National Cheng Kung University, Tainan 701, Taiwan
(Received 7 September 2004; revised manuscript received 1 November 2004; published 3 February 2005)

The precursor phases of $SrFeO_{3-x}$ (SFO) and $SrMoO_4$ (SMO) were used to prepare Sr_2FeMoO_6 with different ratios by a solid-state reaction technique. An x-ray diffractometer was used to identify the phases. SMO was observed to exist in the Mo-rich samples. The high resolution of a transmission electron microscope was employed to identify the compositions and phases. It was further evidenced that Mo-rich nanosized clusters were located inside the grains rather than at grain boundaries. Moreover, the antiphase boundary (APB) was clearly evidenced in the Mo-rich SFMO, which might lead to the Sr- or Fe-rich boundaries. The conduction, magnetic, and magnetotransport properties were characterized, and it was found that the Mo-rich samples had higher resistivity, lower saturated magnetization, and lower coercivity but higher low-field magnetoresistance (LFMR), which was strongly related to the presence of the excess Mo ions and APBs inside the grains. The conduction of SFMO samples with different ratios reveals a semiconductor behavior, which can be described by the VRH model, Eq. (1), with $p=\frac{1}{4}$ and ρ_o independent of temperature in the temperature range of 50 to 300 K. The evaluated values of T_o increase with the decrease of the SFO/SMO ratio, which are considered to be influenced by the residual SMO and APBs inside the grains. It is suggested that the enhancement of LFMR of Mo-rich SFMO is arisen from the APBs or the induced Sr- or Fe-rich grain boundaries.

DOI: 10.1103/PhysRevB.71.064401 PACS number(s): 75.47.Lx, 75.50.Bb, 75.47.Gk, 61.72.Mm

I. INTRODUCTION

Although the lanthanum magnanites possess colossal magnetoresistance (MR), the high applied field and low Curie temperature have hampered their practical uses. The double perovskite Sr_2FeMoO_6 (SFMO), however, possessing an appreciable low-field room-temperature MR and a relatively high Curie temperature (410–450 K),[1,2] has stimulated both fundamental and applied research on the structure and physical properties of this compound. The unique character of SFMO is that it possesses a high spin-polarization of conduction carriers,[1] which is attractive in the light of the potential application to the magnetoresistive devices. The peculiar properties are arisen from the half-metallic density of states in the electronic structure of SFMO.[1,3,4] While there still is argument concerning the valence states of Fe and Mo ions,[5–11] the ions of Fe^{3+} and Mo^{5+} are considered to be dominant. The electronic structure of SFMO was considered as the majority spin band is gapped and the corresponding $3d^5$ spin up electrons localize in the Fe^{3+} ions while the conduction band is partially occupied by the $4d^1$ down spin electrons of Mo^{5+} ions.[1] Such a half-metallic nature gives rise to 100% spin-polarized charge carriers in the ground state. It is believed that the ferrimagnetism originates from the antiferromagnetic coupling between $Fe^{3+}(3d^5;t^3_{2g}e^2_g\uparrow)$ and $Mo^{5+}(4d^1;t^1_{2g}\downarrow)$ ions, which produces a saturated magnetic moment of $4\mu_B$. However, the observed saturation moment by several groups was always $3.1–3.2\mu_B$.[1,3,7,12,13] The low saturation moment was attributed to antisite defects resulting from the partial disorder of Fe-Mo ions among the B/B' sublattices.[3,14]

For the conduction behavior of SFMO, both semiconductive and metallic behaviors were found in the electronic conduction of SFMO, depending on the crystal form, heat treatments, and compositions.[3,6,7,15] The degeneracy of the two states of Fe^{3+}-Mo^{5+} and Fe^{2+}-Mo^{6+} had been observed[11] and suggested as the origin of the metallic behavior.[6] The semiconducting behavior was usually attributed to the presence of the inhomogeneous compositions or phases in the grain boundary.

SFMO possesses an appreciable low-field magnetoresistance (LFMR) in the granular form.[1] Because very weak MR was observed in the single crystal,[3] LFMR of SFMO was usually considered to be related to the grain boundary.[1,2,16–24] With few exceptions, most models for the grain-boundary MR were based on the spin-polarized tunneling (SPT).[25] Basically, the barrier at or near the grain boundary was assumed to be insulating or nonferromagnetic in the SPT model.[26] However, for the manganese perovskite, grain-boundary magnetization (GBM) had been observed and suggested to play a crucial role in LFMR.[27–36] While the mechanism of LFMR was intensively studied in the manganese perovskite,[25,27–39] it was not for SFMO. The enhancement of LFMR of SFMO was recently reported to be related to the nonmagnetic SMO phase residing at the grain boundary.[19,40] However, there was no microstructural evidence showing the SMO phase at the grain boundary. Actually, the report by Sharma *et al.*[21] and our previous work[41] have evidenced that the enhancement of LFMR of SFMO is not related to the grain-boundary phases. Moreover, there was a striking observation that the MR was weak across artificial grain boundaries in epitaxial thin films grown on bicrystalline substrates[16] and the antisite disorder has been suggested to be related to the LFMR.[42] Though the antiphase boundary (APB) was found to cause a large MR in magnetite,[43] it was reported to be scarcely observed in SFMO.[44] In this investigation, we not only showed the absence of SMO phase at the grain boundary but also provided the clear evidence of the presence of the APB. The possible roles of SMO and APB in the conduction and the LFMR enhancement of SFMO were pursued.

II. EXPERIMENT

The formation mechanism of Sr_2FeMoO_6 (SFMO) had been detailed in the previous works,[45,46] which suggested that formation of SFMO could be via the reaction of $SrFeO_{3-x}$ (SFO) and $SrMoO_4$ (SMO). Thus, different ratios of SFO/SMO, i.e., 1:1, 0.9:1, and 0.8:1 had been selected to prepare SFMO. The mixture was sintered at 1200 °C for 4 h in 5% H_2-95% N_2. An x-ray diffractometer (Model D/MAX III.V, Ragaku Co., Tokyo, Japan) was used to identify phases. A high resolution transmission electron microscope (HRTEM) (JEM-100CXII, JEOL, Japan) equipped with an energy dispersive x-ray (EDX) spectrometer was used to identify the compositions and phases. A multimeter (Model 2001/MEM2, Keithley Instruments Inc., Cleveland, OH) was used to measure the electrical resistivity over a range of $50 \leqq T \leqq 300$ K. The magnetization was measured by a superconducting quantum interference device magnetometer (Model MPMS/MPMS2, Quantum Design Inc., San Diego, CA), which was performed under a fixed field of 10 KOe using the zero field cooling method. The magnetoresistivity (MR) was measured by the standard four-probe method in the external magnetic fields. The MR was evaluated by the following equation:

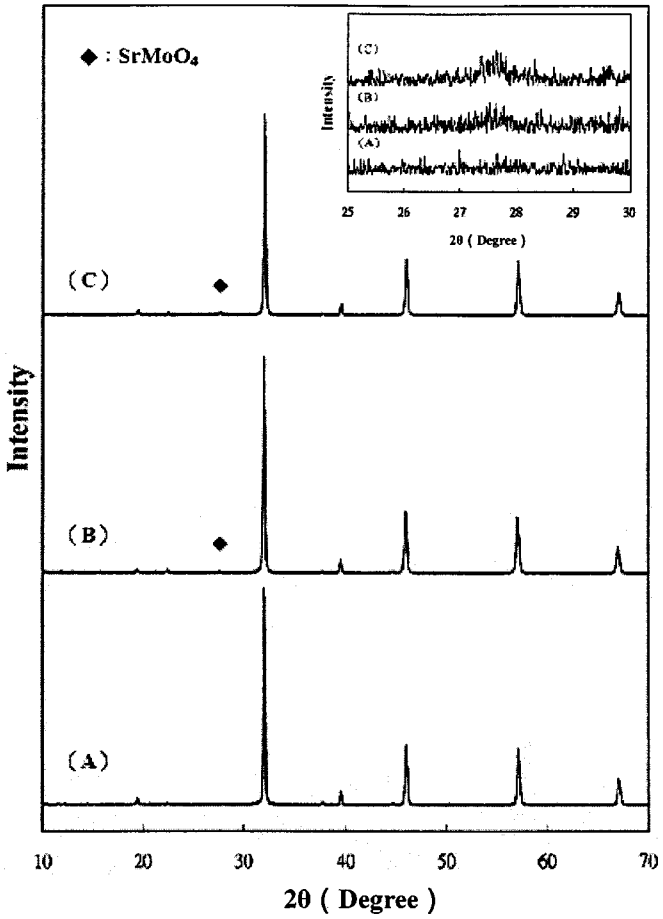

FIG. 1. Comparison of x-ray patterns of polycrystalline Sr_2FeMoO_6 samples prepared by different ratios of $SrFeO_{3-x}/SrMoO_4$ (a) 1:1, (b) 0.9:1, and (c) 0.8:1.

$$\mathrm{MR}(\%) = [(R_H - R_0)/R_0] \times 100\,\%\,,$$

where R_H is the resistivity measured under the field and R_0 is the resistivity measured without the field.

III. RESULTS AND DISCUSSION

A. X-ray and TEM investigations

Figure 1 shows the comparison of the x-ray patterns of polycrystalline SFMO samples with different ratios of SFO/SMO sintered at 1200 °C for 4 h in 5% H_2–95% N_2. It was observed that the residual phase of SMO increased with the SFO/SMO ratio. The residual SMO was considered to be located along the grain boundary.[19,40] However, recently, it has been suggested that SMO is located inside the grains rather than at the grain boundaries.[41] Here, we provide more evidence to further justify that SMO is indeed present inside the grains. Figure 2 shows the micrographs of the HRTEM revealing the presence of Mo-rich nanosized clusters inside the grains of the Mo-rich SFMO samples. The compositions of grains, grain boundaries, and the nanosized clusters of SFMO with different SFO/SMO ratios were listed in Table I. It clearly indicates that the grain boundaries are relatively Sr rich or Fe rich, and the nanosized clusters inside the grains are Mo rich. Thus, the residual SMO should be present in the grains rather than at grain boundaries. These results are also supported by the previous proposed formation mechanism of SFMO,[45,46] indicating that there would be less chance for SMO to locate at the grain boundaries. Moreover, the alternate black/white fringes characterizing the image of APB had been frequently observed in the Mo-rich samples, shown in Fig. 3. This further supports the presence of the excess ions inside the grains because if more Mo ions present inside the grains, the order states of Fe and Mo ions would be disturbed and the occurrence of the APB becomes possible.

B. Effect of residual SMO and APB on the conduction behavior

Figure 4 shows the conduction behavior at different temperatures for the samples with different SFO/SMO ratios. As observed, they show the semiconductive behavior, and the resistivity of the samples with SMO is higher than that without SMO. Though the temperature dependence of the conduction behavior of single-crystal SFMO was found to be a metallic behavior,[1] the polycrystalline samples in general show a semiconductive behavior depending on the sample preparation.[7,15] Itoh *et al.*[7] reported that polycrystalline SFMO sample could be made metallic and had lower resistivity by postannealing in vacuum-sealed quartz tubes (for 72 h at 1373 K), which was attributed to the improvement of conductivity of the grain-boundary phase or to the homogenization of the composition of the sample, whereas Chmaissem *et al.*[15] reported that the sample with higher molar fraction of SMO possessed lower resistivity and revealed metallic behavior but that with lower or without SMO had higher resistivity and showed a semiconducting behavior. The above results seem to be contradicted to each other. However, the observation by Asano *et al.*[47] provides a rea-

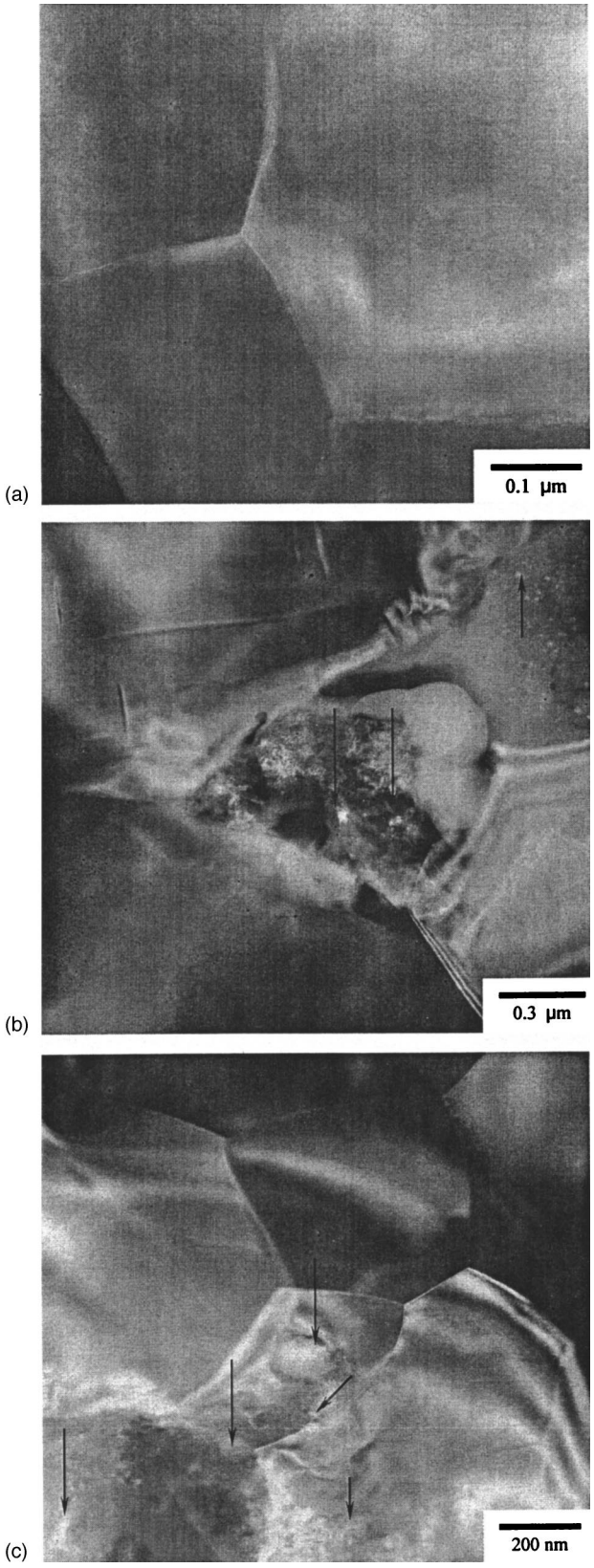

FIG. 2. The comparison of HRTEM micrographs of Sr_2FeMoO_6 with different ratios of $SrFeO_{3-x}/SrMoO_4$ (a) 1:1, (b) 0.9:1, and (c) 0.8:1, showing the existence of Mo-rich nanosized clusters, indicated by arrows, and the average compositions of grains, grain boundaries, and nanosized clusters were examined by EDX and listed in Table I.

TABLE I. The average compositions of grains, grain boundaries, and nanosized clusters in Fig. 3, examined by EDX.

		Element (Atom %)		
		Sr	Fe	Mo
1:1	Grain	52.72	22.11	25.17
	Boundary	51.45	23.18	24.41
0.9:1	Grain	52.52	19.96	27.52
	Boundary	52.95	23.75	23.3
	Nano-sized clusters	56.69	12.49	30.82
0.8:1	Grain	49.67	19.64	30.69
	Boundary	53.95	21.03	25.02
	Nano-sized clusters	54.83	10.81	34.36

sonable interpretation about this contradiction.

In their epitaxial films free from bulk grain boundaries, Asano *et al.*[47] showed that the sample with nanoclusters (size about 10–15 nm) had much higher resistivity and a characteristic of a semiconductor but that with coarsened clusters of a size over 100 nm revealed lower resistivity and metallic behavior. Apparently, the morphology of the second phase including size, distribution, and location would play a significant role in conduction behavior of SFMO. It should be noted that the resistivity of the sample with SMO is still very low $<100\ \Omega$ cm compared with the common ceramics. If the insulating SMO would be located along the grain boundary, the resistivity would become very high. Therefore, the great enhancement of the resistivity of SFMO can be attributed to the fact that the nanosized clusters of SMO inside the grains disturb the intrinsic conduction mechanism of SFMO. It was known that for the sample with the SFO/SMO ratio of 1:1, the single-phase SFMO would only be produced in a reducing atmosphere and SMO would be present when sintered in air.[45,46] Therefore, the long-time heat treatment of the raw powders of SFMO in air would lead to the coarsening of the particle sizes of SFMO and SMO, which in turn would profound the morphology of SMO and the microstructure of SFMO in the final sintered body. This may be a possible reason to explain the conduction behavior of the samples reported by Chmaissem *et al.*[15]

While the origin of the conduction mechanism of SFMO is still ambiguous, the semiconducting behavior of $Sr_2Fe_xMo_{2-x}O_6$ $(1.2 \leqslant x \leqslant 1.5)$ has been suggested to be fit for polaron hopping model.[48] If polaron motion indeed is dominant in the conduction mechanism of SFMO, the APB and nanosized clusters would play a significant role in the conduction mechanism because they could affect the lattice vibration mode and ordering of Fe-Mo ions. Figure 5 shows the fitting of the variable range hopping model of SFMO with different SFO/SMO ratios. The general governed equation based on the hopping charge transfer can be written as[49]

$$\rho(T) = \rho_o \exp[(T_o/T)^p], \tag{1}$$

where T_o is a characteristic temperature and $p=1$ for hopping over the nearest sites,[50] $p=\frac{1}{4}$ for the Mott[49] variable-range hopping (VRH) models and $p=\frac{1}{2}$ for the Shklovskii-Efros[51]

(SE) VRH model. Moreover, $T_o = Qa^{1-1/p}$, where a is the localization radius of charge carriers and $Q = \alpha/[kg(E_f)]$, where $\alpha = 18$, $g(E_f)$ is the density of localized states (DOS) at the Fermi level, and E_f is the Fermi level. When the Coulomb interaction between the hopping carrier is unimportant, $p = \frac{1}{4}$. In the opposite case, the Coulomb interaction creates a soft parabolic gap with width Δ in the DOS around E_f, which gives $p = \frac{1}{2}$. If $\Gamma = [kT(T_o/T)^p a/(2\hbar s)]^2 \ll 1$ (s is the sound velocity), the dependence of ρ_o on T is weak and can be neglected. For $\Gamma \gg 1$, the prefactor is given by the equation $\rho_o = AT^m$, depending on the phonon density, where A is a constant. For the SE mechanism, $m = \frac{9}{2}$ or $\frac{5}{2}$ and for Mott VRH conductivity, $m = \frac{25}{4}$ or $\frac{21}{4}$. After fitting all the possible VRH models mentioned above for the conductivity data at temperatures above T_c, it was found that the best fit was the VRH model with $p = \frac{1}{4}$ and ρ_o independent of temperature in the temperature range of 50 to 300 K, shown in Fig. 5. The evaluated values of the parameter, T_o, have been listed in the Table II, showing that they increase with the decrease of the SFO/SMO ratio. In Ref. 52, T_o was found to be related to the measure of the extent of the disordering state of the material. Thus, the increasing values of T_o for the Mo-rich samples are clearly influenced by the ordering states of Mo and Fe ions due to the presence of the excess Mo ions and APBs inside the grains.

C. Effect of residual SMO and APB on the magnetic and magnetotransport properties

Figure 6 shows the magnetization as a function of temperature for the samples with and without the residual phase of SMO. As observed, the samples with SMO have a lower magnetization at each temperature. The magnetization ob-

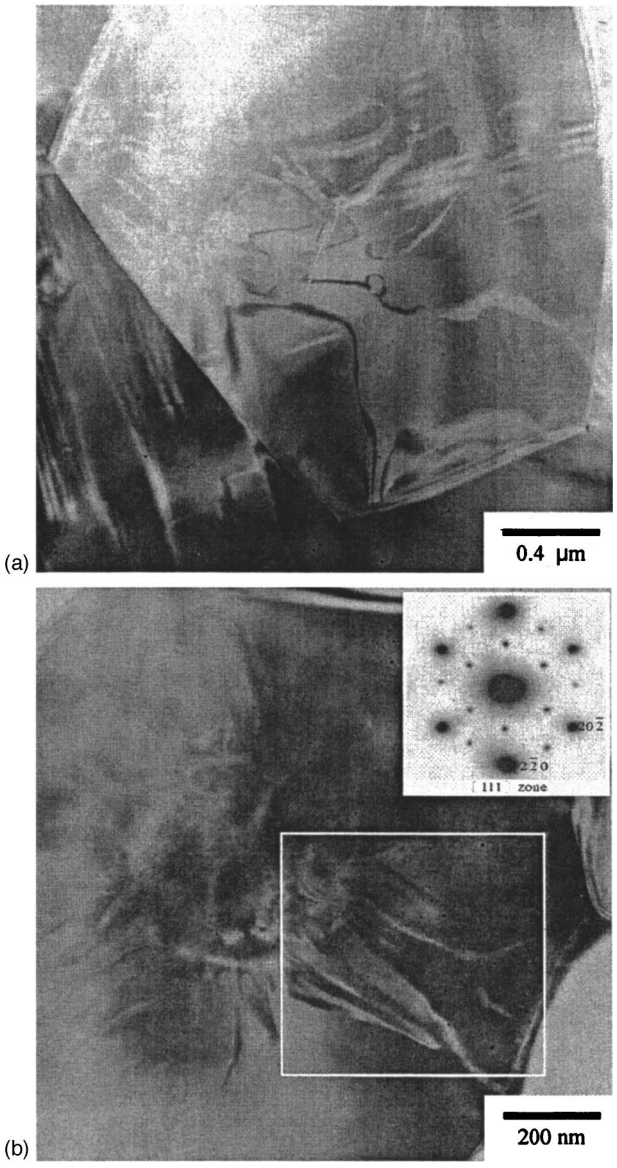

FIG. 3. HRTEM micrographs of Mo-rich Sr_2FeMoO_6 with $SrFeO_{3-x}/SrMoO_4$ ratios of (a) 0.9:1 and (b) 0.8:1, showing the presence of antiphase boundaries.

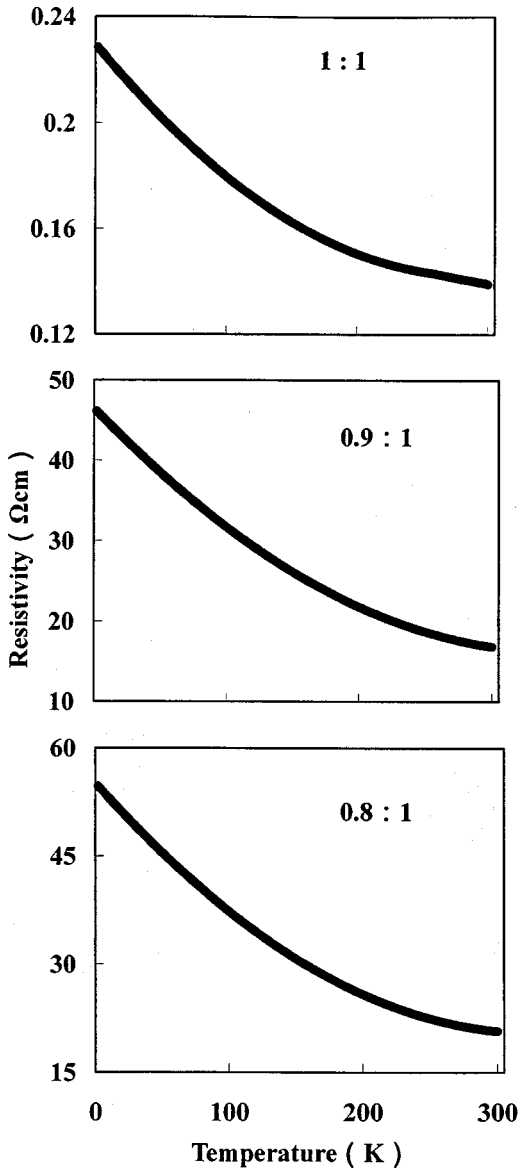

FIG. 4. Temperature dependence of the resistivity ρ for Sr_2FeMoO_6 with different $SrFeO_{3-x}/SrMoO_4$ ratios.

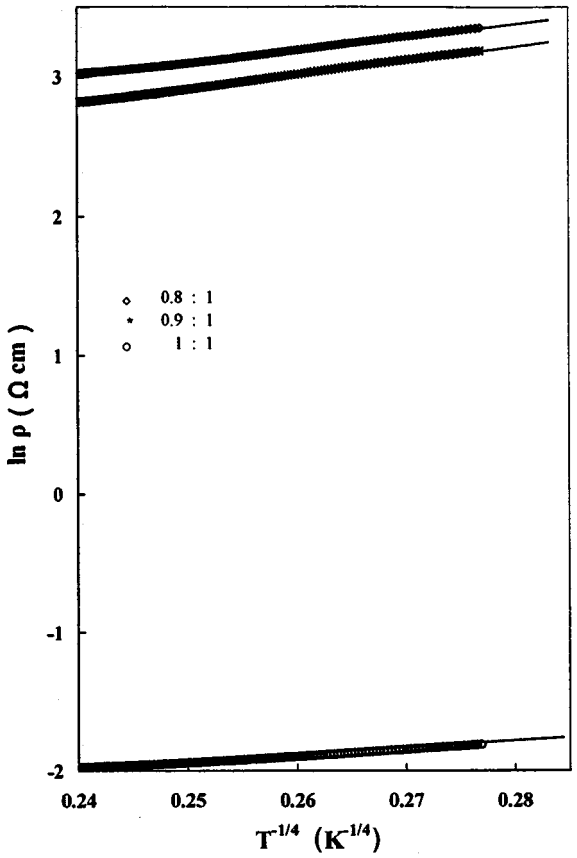

FIG. 5. The resistivity as a function of temperature showing that the best fit was the VRH model, Eq. (1), with $p=\frac{1}{4}$ and ρ_o independent of temperature for Sr_2FeMoO_6 with different $SrFeO_{3-x}$/$SrMoO_4$ ratios in the temperature range from 50 to 300 K.

tained for the samples of SFMO are $2.9\mu_B$, $2.5\mu_B$, and $2.2\mu_B$ for the SFO/SMO ratios of 1, 0.9, and 0.8, respectively. The lower magnetization of the Mo-rich samples would arise from the disorder of the *B* site arrangement[14] and the presence of the nonmagnetic phase SMO, which is strongly related to the excess Mo ions and APB inside the grains, is observed in Figs. 2 and 3. Moreover, Fig. 7 shows the M-H hysteresis loop of the SFMO samples with different SFO/SMO ratios, in which the Mo-rich samples reveal the unusual characteristics: a low saturation magnetization, a remarkable low remanence, and a small coercivity, which could be attributed to presence of the APBs inside the grains.[16]

Figure 8 shows the comparison of MR as a function of the magnetic field for the SFMO samples with different SFO/SMO ratios at 100 and 300 K. The result shows that the

TABLE II. The evaluated values of the parameters of T_o and ρ_o in Eq. (1) for Sr_2FeMoO_6 with different $SrFeO_{3-x}$/$SrMoO_4$ ratios in the temperature range from 50 to 300 K.

	1:1	0.9:1	0.8:1
T_o	427	7050	11 347
ρ_o	0.046	1.397	2.251

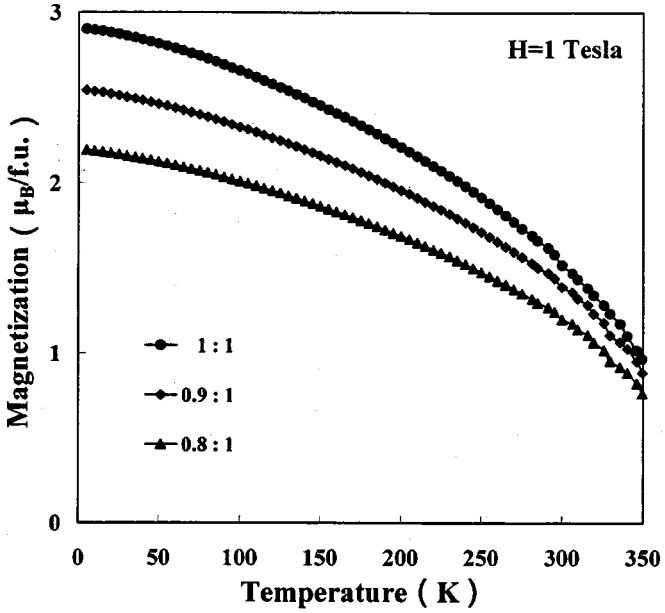

FIG. 6. M-H hysteresis loops of Sr_2FeMoO_6 with different $SrFeO_{3-x}$/$SrMoO_4$ ratios.

Mo-rich SFMO samples have higher MR. The enhancement of the LFMR of SFMO was usually attributed to the SMO located at the grain boundary.[19,40] However, so far, it has not been justified by the microstructural evidence. In Ref. 41 and this investigation, we have shown that SMO is essentially not located at the grain boundary. If SMO is not located at the grain boundaries, there seems to be another mechanism in enhancing the LFMR of Mo-rich SFMO. In this investigation, the presence of the APBs is clearly evidenced, shown in Fig. 3. Based on the recent study in Ref. 43 about the influence of APBs on the MR in thin films of Fe_3O_4, the influ-

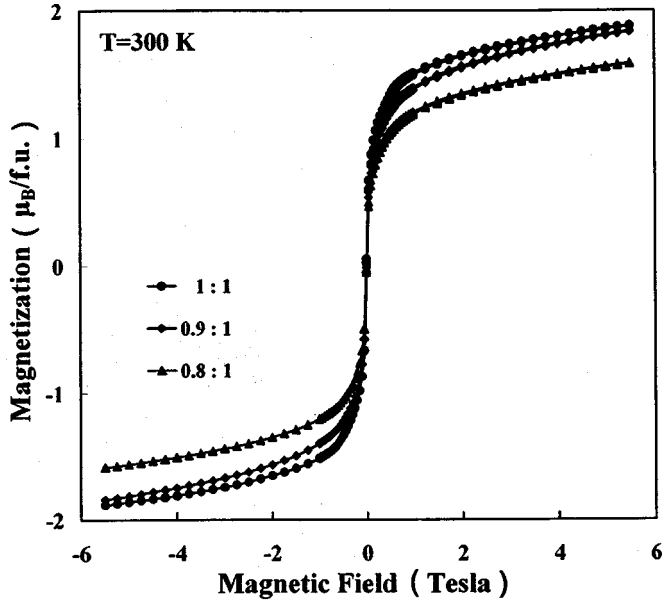

FIG. 7. Magnetization (M) as a function of temperature under a field of 10 K Oe for samples with different ratios of $SrFeO_{3-x}$/$SrMoO_4$.

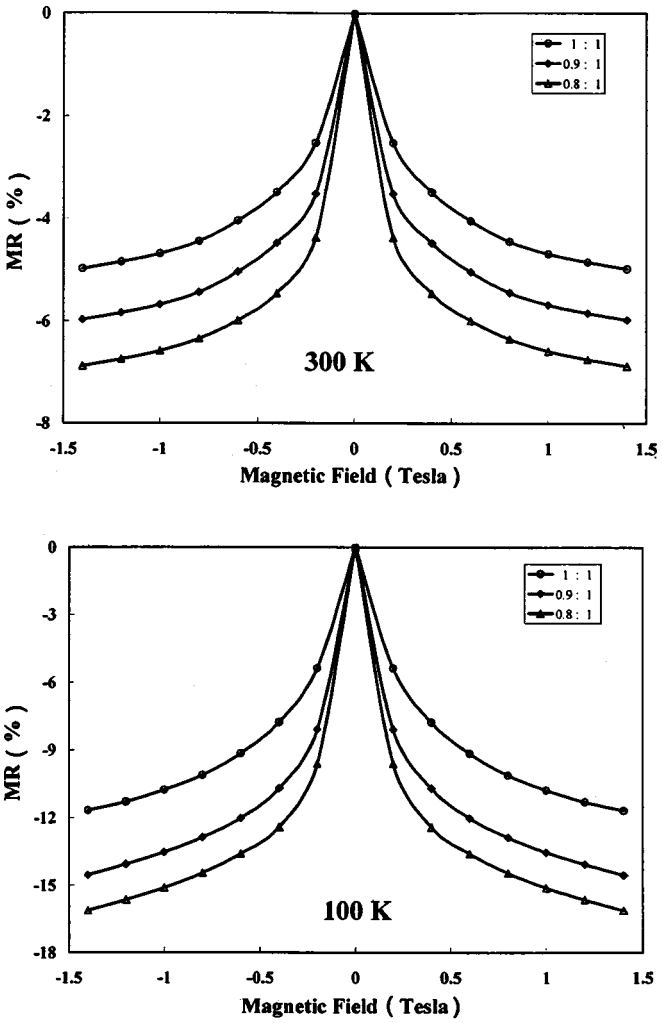

FIG. 8. Magnetoresistivity ratio (MR %) as a function of the applied field for Sr_2FeMoO_6 with different $SrFeO_{3-x}/SrMoO_4$ ratios at 100 and 300 K.

ence of the APB *per se* on the LFMR cannot be excluded. Moreover, recent reports[53] have suggested that the doping ions or the oxygen content rather than second phases in the grain boundaries would have a great influence on the grain boundary resistivity and MR. Table I shows the results of the compositional analyses in grains and grain boundaries of the SFMO samples with different SFO/SMO ratios, revealing that the grain boundaries are Sr rich or Fe rich. Thus, an alternative mechanism for the enhancement of the LFMR and resistivity for the Mo-rich samples may also be possible, namely, the development of the Sr- or Fe-rich grain boundaries due to the presence of the APBs based on the Mo ions. However, it needs more work to further clarify this mechanism.

IV. CONCLUSIONS

Mo-rich nanosized clusters and APBs were clearly evidenced inside the grains of the Mo-rich Sr_2FeMoO_6 (SFMO) samples. Mo-rich SFMO has lower saturated magnetization, higher resistivity, lower coercivity, and higher low-field magnetoresistivity, which are related to the excess Mo ions and APBs inside the grains. The conduction of SFMO samples with different ratios reveals a semiconductor behavior, which can be described by the VRH model, Eq. (1), with $p=\frac{1}{4}$ and ρ_o independent of temperature in the temperature range of 50 to 300 K. The evaluated values of T_o increase with the decrease of the SFO/SMO ratio, which are influenced by the ordering states of Mo and Fe ions due to the presence of the excess Mo ions and APBs inside the grains. It is suggested that APBs or the induced Sr- or Fe-rich grain boundaries may be a possible reason for the enhancement of LFMR and resistivity in the Mo-rich SFMO samples.

ACKNOWLEDGMENTS

The author appreciates the financial support from the National Science Council of Taiwan, ROC, under Contract No. NSC91-2216-E-006-032.

*Electronic address: ttfang@mail.ncku.edu.tw

[1] K.-I. Kobayashi, T. Kimura, H. Sawada, K. Terakura, and Y. Tokura, Nature (London) **395**, 677 (1998).
[2] T. H. Kim, M. Uehara, S. W. Cheong, and S. Lee, Appl. Phys. Lett. **74**, 1737 (1999).
[3] Y. Tomioka, T. Okuda, Y. Okimoto, R. Kumai, and K.-I. Kobayashi, Phys. Rev. B **61**, 422 (2000).
[4] T. Saitoh, M. Nakatake, A. Kakizaki, H. Nakajima, O. Morimoto, S. Xu, Y. Moritomo, N. Hamada, and Y. Aiura, Phys. Rev. B **66**, 035112 (2002).
[5] S. Nakayama, T. Nakagawa, and S. Nomura, J. Phys. Soc. Jpn. **24**, 219 (1968).
[6] A. W. Sleight and J. F. Weiher, J. Phys. Chem. Solids **33**, 679 (1972).
[7] M. Itoh, I. Ohta, and Y. Inaguma, Mater. Sci. Eng., B **41**, 55 (1996).
[8] B. García-Landa, C. Ritter, M. R. Ibarra, J. Blasco, P. A. Algarabel, R. Mahendiran, and J. García, Solid State Commun. **110**, 435 (1999).
[9] D. Niebieskikwiat, R. D. Sánchez, A. Caneiro, L. Morales, M. Vásquez-Mansilla, F. Rivadulla, and L. E. Hueso, Phys. Rev. B **62**, 3340 (2000).
[10] M. S. Moreno, J. E. Gayone, M. Abbate, A. Caneiro, D. Niebieskikwiat, R. D. Sánchez, A. de Siervo, R. Landers, and G. Zampieri, Solid State Commun. **120**, 161 (2001).
[11] J. H. Kim, S. C. Wi, S. Yoon, B. J. Suh, J. S. Kang, S. W. Han, K. H. Kim, A. Sekiyama, S. Kasai, S. Suga, C. Hwang, C. G. Olson, B. J. Park, and B. W. Lee, J. Korean Phys. Soc. **43** (3), 416 (2003).
[12] Y. Morimoto, S. Xu, A. Machida, T. Akimoto, E. Nishibori, M. Takata, and M. Sakata, Phys. Rev. B **61**, R7827 (2000).
[13] T. Nakagawa, J. Phys. Soc. Jpn. **24**, 806 (1968).

[14] A. S. Ogale, S. B. Ogale, R. Ramesh, and T. Venkatesan, Appl. Phys. Lett. **75**, 573 (1999).
[15] O. Chmaissem, R. Kruk, B. Dabrowski, D. E. Brown, X. Xiong, S. Kolesnik, J. D. Jorgensen, and C. W. Kimball, Phys. Rev. B **62**, 14 197 (2000).
[16] H. Q. Yin, J. S. Zhou, J. P. Zhou, R. Dass, J. T. McDevitt, and J. B. Goodenough, Appl. Phys. Lett. **75** (18), 2812 (1999).
[17] J. P. Zhou, R. Dass, H. Q. Yin, J. S. Zhou, L. Rabenberg, and J. B. Goodenough, J. Appl. Phys. **87** (9), 5037 (2000).
[18] H. Q. Yin, J. S. Zhou, R. Dass, J. P. Zhou, J. T. McDevitt, and J. B. Goodenough, J. Appl. Phys. **87** (9), 6761 (2000).
[19] D. Niebieskikwiat, A. Caneiro, R. D. Sanchez, and J. Fontcuberta, Phys. Rev. B **64**, 180406 (2002).
[20] D. Niebieskikwiat, A. Caneiro, R. D. Sánchez, and J. Fontcuberta, Physica B **320**, 107 (2002).
[21] A. Sharma, A. Berenov, J. Rager, W. Branford, Y. Bugosiavsky, L. F. Cohen, and J. L. MacManus-Driscoll, Appl. Phys. Lett. **83** (12), 2384 (2003).
[22] K. Wang and Y. Sui, Solid State Commun. **129**, 135 (2004).
[23] K. Wang and Y. Sui, Physica B **344**, 423 (2004).
[24] C. L. Yuan, Y. Zhu, P. P. Ong, Z. X. Shen, and C. K. Ong, Solid State Commun. **129**, 551 (2004).
[25] H. Y. Hwang, S. W. Cheong, N. P. Ong, and B Batlogg, Phys. Rev. Lett. **77**, 2041 (1996).
[26] M. Jullière, Phys. Lett. **54A**, 225 (1975).
[27] A. Gupta, G. Q. Gong, G. Xiao, P. R. Duncombe, P. Lecoeur, P. Trouilloud, Y. Y. Wang, V. P. Dravid, and J. Z. Sun, Phys. Rev. B **54**, R15 629 (1996).
[28] N. D. Matthur, G. Burnell, S. P. Isaac, T. J. Jackson, B.-S. Teo, J. L. McManus Driscoll, L. F. Cohen, J. E. Evetts, and M. G. Blamire, Nature (London) **387**, 266 (1997).
[29] K. Steenbeck, T. Eick, K. Kirsch, K. O'Donnell, and E. Seinbeiss, Appl. Phys. Lett. **71**, 968 (1997).
[30] K. Steenbeck, T. Eick, K. Kirsch, H.-G. Schmidt, and E. Seinbeiss, Appl. Phys. Lett. **73**, 2506 (1998).
[31] N. K. Todd, N. D. Mathur, S. P. Isaac, J. E. Evetts, and M. G. Blamire, J. Appl. Phys. **85**, 7263 (1999).
[32] R. Gross, L. Alff, B. Büchner, B. H. Freitag, C. Höfener, J. Klein, Y. Lu, W. Mader, J. B. Philipp, M. S.R. Rao, P. Reutler, S. Ritter, S. Thien haus, S. Uhlenbruck, and B. Wiedenhorst, J. Magn. Magn. Mater. **211**, 150 (2000).
[33] C. Höfener, J. B. Philip, J. Klein, L. Alff, A. Marx, B. Büchner, and R. Gross, Europhys. Lett. **50**, 681 (2000).
[34] R. Mathieu, P. Svedlindh, R. Gunnarsson, and Z. G. Ivanov, Phys. Rev. B **63**, 132407 (2001).
[35] A. Glaser and M. Ziese, Phys. Rev. B **66**, 094422 (2002).
[36] R. Gunnarsson, A. Kadigrobov, and Z. Ivanov, Phys. Rev. B **66**, 024404 (2002).
[37] J. Klein, C. Hoffner, S. Uhlenbruck, L. Alff, B. Buchner, and R. Gross, Europhys. Lett. **47**, 371 (1999).
[38] J. E. Evetts, N. D. Mathur, S. P. Isaac, B. S. Teo, L. F. Cohen, J. L. MacManus-Driscoll, and M. G. Blamire, Philos. Trans. R. Soc. London, Ser. A **356**, 1593 (1998).
[39] A. Glaser and M. Ziese, Phys. Rev. B **66**, 094422 (2002).
[40] C. L. Yuan, Y. Zhu, and P. P. Ong, Appl. Phys. Lett. **82**, 934 (2003).
[41] Tsang-Tse Fang and J. C. Lin, J. Am. Ceram. Soc. **87**, 1343 (2004).
[42] J. Navarro, Ll. Balcells, F. Sandiumenge, M. Bibes, A. Roig, B. Martínez, and J. Fontcuberta, J. Phys.: Condens. Matter **13**, 8481 (2001).
[43] W. Eerenstein, T. T. M. Palstra, S. S. Saxena, and T. Hibma, Phys. Rev. Lett. **88**, 247204 (2002).
[44] J. Lindén, Phys. Rev. B **68**, 174415 (2003).
[45] Tsang-Tse Fang, M. S. Wu, and T. F. Ko, J. Mater. Sci. Lett. **20**, 1609 (2001).
[46] Tsang-Tse Fang and T. F. Ko, J. Am. Ceram. Soc. **86** (9), 1453 (2003).
[47] H. Asano, S. B. Ogale, J. Garrison, A. Orozzco, Y. H. Li, E. Li, V. Smolyaninova, C. Galley, M. Downes, M. Rajeswari, R. Ramesh, and T. Venkatesan, Appl. Phys. Lett. **74** (24), 3696 (1999).
[48] G. Y. Liu, G. H. Rao, X. M. Feng, H. F. Yang, Z. W. Ouyang, W. F. Liu, and J. K. Liang, Physica B **334**, 229 (2003).
[49] N. F. Mott and E. A. Davies, *Electron Processes in Non-Crystalline Materials* (Clarendon, Oxford, 1979); N. F. Mott, *Metal-Insulator Transition* (Taylor and Francis, London, 1990).
[50] T. Holstein, Ann. Phys. (N.Y.) **8**, 343 (1959).
[51] B. I. Shklovskii and A. L. Efros, *Electronic Properties of Doped Semiconductors* (Springer, Berlin, 1984).
[52] T.-T. Fang, E. Lu, and H.-F. Ho, J. Am. Ceram. Soc. (to be published).
[53] M. G. Blamire, C. W. Schneider, G. Hammerl, and J. Annhart, Appl. Phys. Lett. **82**, 2670 (2003).